Journal of Power Sources 196 (2011) 495–503

Contents lists available at ScienceDirect

Journal of Power Sources

journal homepage: www.elsevier.com/locate/jpowsour

Differences in the effects of Co and CoO on the performance of $Ni(OH)_2$ electrode in Ni/MH power battery

Yang Xia, Yifu Yang*, Huixia Shao

College of Chemistry and Molecular Science, Wuhan University, Wuhan 430072, PR China

ARTICLE INFO

Article history:
Received 15 March 2010
Received in revised form 25 May 2010
Accepted 21 June 2010
Available online 25 June 2010

Keywords:
Ni/MH power battery
Cobalt oxide
Cobalt
Electro-oxidation
Conductive network

ABSTRACT

The effects of metallic cobalt (Co) and cobalt monoxide (CoO), as additives in positive electrodes, on the electrochemical performance of nickel/metal hydride (Ni/MH) power batteries are studied. Commercial Co and CoO are charged at 50 °C in 6 M KOH solution. The oxidation mechanism of cobalt materials is investigated by observing structural and morphological evolutions during charging. A pure Co_3O_4-type phase is formed when the starting material is CoO. When Co is used, a cobalt oxyhydroxide (CoOOH) phase is present, together with a tricobalt tetroxide (Co_3O_4) phase. In both cases, the cobalt concentration in the electrolyte decreases during oxidation. The final product is dependent on the solubility of cobalt and the kinetics of the reaction that consumes cobalt tetrahydroxide $[Co(OH)_4]^{2-}$. The highly compact CoOOH phase, which works well between the nickel foam frame and nickel hydroxide $[Ni(OH)_2]$ particles, enhances the power performance of Ni/MH power battery. The Co_3O_4 phase, which works well in connecting $Ni(OH)_2$ particles, improves the capacitive performance of Ni/MH power battery.

1. Introduction

Nickel/metal hydride (Ni/MH) power battery is considered as one of the most promising devices for electric vehicle (EV) and hybrid electric vehicle (HEV) applications [1]. However, a power battery has to satisfy essential requirements, the most important of which are the: (1) low internal resistance and (2) high rate charge and discharge capability of the active materials. Both nickel hydroxide $[Ni(OH)_2]$ and its oxidized form (NiOOH) are very poor in electrical conduction, so the direct use of active materials in power batteries is almost impossible. To solve this problem, different forms of cobalt are used as additives in the positive electrode to improve the conductivity of $Ni(OH)_2$ [2]. Cobalt additives are normally added by co-precipitation and post-addition methods [3].

When cobalt is co-precipitated with nickel into the active mass, the cells show a maximum capacity at a cobalt content of 11% [4]. In the case of post-addition, cobalt phases form a conductive network after the first charging to form an electrical connection between the $Ni(OH)_2$ particles and the current collector [5]. Although most previous studies have focused on the performance of the $Ni(OH)_2$ electrode, some studies have demonstrated the use of cobalt additives to enable redox chemistry in an alkaline medium. Benson et al. studied the electrochemical behavior of cobalt compounds in alkaline solutions and showed that cobalt hydroxide/oxyhydroxide $[Co(OH)_2/CoOOH]$ redox has poor electrochemical reversibility [6]. More recently, studies showed that the non-stoichiometric H_xCoO_2 phase was the conductive phase, rather than the stoichiometric CoOOH, which is a poor conductor [7].

Moreover, the final product of adding cobalt to $Ni(OH)_2$ electrodes depends strongly on the charge rate [3]. For instance, high charging rates favored the formation of the conducting H_xCoO_2 phase [8]. In contrast, low charging rates facilitated easier formation of a CoOOH phase [7,9]. Another important property of cobalt materials is their solubility in concentrated alkaline media. In the post-addition method, the cobalt monoxide (CoO) additive is hydrolyzed into $Co(OH)_2$. This dissolution-reprecipitation process results in the uniform distribution of cobalt in the positive electrode [5,10]. Thus, the addition of CoO produces a better product than the direct addition of $Co(OH)_2$. Despite the many advantages, the post-addition of CoO has drawbacks. Cobalt can be reduced, and it tends to move from the whole electrode to the surface of a current collector [8,11], thereby decreasing the cell performance when the cell is stored in a discharged state [12,13].

To improve the stability of the conductive network, Ni/MH batteries are normally activated by an initial charge at 40–80 °C to promote the formation of the cobalt conductive networks [14,15].

* Corresponding author. Tel.: +86 27 62475962; fax: +86 27 68754067.
E-mail address: yang-y-f1@vip.sina.com (Y. Yang).

0378-7753/$ – see front matter © 2010 Elsevier B.V. All rights reserved.
doi:10.1016/j.jpowsour.2010.06.065

In these conditions, cobalt additives tend to form a material similar to a tricobalt tetroxide (Co_3O_4) spinel phase. This is different from the ideal Co_3O_4 and has good conductivity and stability [16]. Tronel et al. studied the formation mechanism of Co_3O_4 and showed that high temperature is an important condition in the formation of Co_3O_4, which is similar to the case of the spinel phase [17]. The electronic conductivity of the cobalt spinel phase can also be improved by thermal treatment [18].

Considering that the first charging condition is similar to the industrial process, this result has raised the issue of the possible use of this particular cobalt phase in Ni/MH power batteries [14,15]. Therefore, understanding the detailed structural and textural evolutions of cobalt additives during charging at elevated temperatures and their effects on power batteries has both academic and technical significance.

In this study, metallic cobalt (Co) and CoO were post-added to $Ni(OH)_2$ electrodes, and the corresponding Ni/MH power batteries were assembled. The effects of the two additives on the performance of the power batteries were compared. Simulating the charge condition of power batteries, the behavior of Co and CoO was investigated during the charge at 50 °C in KOH solutions. Investigation focused on structural and morphological evolutions. The presence of cobalt species in the electrolyte and its concentration evolution during electro-oxidation were studied as well. Finally, the electro-oxidation mechanism of Co and CoO was proposed as an explanation for their indispensable effects on the performance of power batteries.

2. Experimental

2.1. Preparation of Ni/MH power batteries and test procedure

Two kinds of positive electrodes were made by filling nickel foam substrates with a mixture of commercially available reagents: (1) 1 wt% polytetrafluoroethylene (PTFE) binder, 10 wt% CoO, and 89 wt% β-$Ni(OH)_2$; and (2) 1 wt% PTFE binder, 8 wt% Co, and 91 wt% β-$Ni(OH)_2$. Both were dried and pressed. The same amounts of β-$Ni(OH)_2$ and cobalt element were used in each positive electrode. Lanthanum-nickel ($LaNi_5$)-based commercial negative MH electrodes were used. Negative and positive electrodes were assembled with a polypropylene separator to form prismatic batteries with a capacity of 5.8 Ah. The batteries were then sealed. The electrolyte used was 6 M KOH solution. The only difference between the two kinds of Ni/MH power batteries was the additives of the positive electrode. Batteries with CoO and Co additives were named CoO-added batteries and Co-added batteries, respectively.

The ready-made batteries were placed at 50 °C for 4 h and then charged at 0.02 C for 50 h. Subsequently, they were activated by charging at 0.2 C for 5 h and discharging at 0.2 C to a cut-off voltage of 1.0 V for 8 cycles at 20 °C. A rate of 1 C corresponds to the current needed to discharge the total capacity of the batteries in 1 h. A cycling test was performed on the batteries by charging at 0.5 C for 2 h and discharging at 0.5 C to a cut-off voltage of 1.0 V to determine the practical capacity.

The batteries were charged at 1 C to the capacity of 5.8 Ah and discharged at 30 C to a cut-off voltage of 0.7 V. This was followed by discharging at 0.5 C to a cut-off voltage of 1.0 V. Charge/discharge studies were conducted with two battery testing equipments (Land Test Equipment, CT2001A; Arbin Test Equipment, BT-2000).

To affirm the nature of the conductive networks in the $Ni(OH)_2$ electrode, the positive electrodes of the two kinds of Ni/MH power batteries were analyzed by scanning electron microscopy (SEM) after testing. Because β-$Ni(OH)_2$ compactly filled the nickel foam together with the cobalt additives and PTFE binder after high pressure pressing, detailed information in the area around the nickel foam could not be visualized by SEM. To solve this problem, a positive electrode with the same composition as that of the tested power battery was again prepared and compressed with a lower pressure. The positive electrode was then assembled with two negative electrodes to form a test cell. The Co-added and CoO-added test cells were charged at 50 °C and activated at room temperature. After these tests, cells were dismantled and the positive electrodes were recovered for SEM characterization.

2.2. Preparation of cobalt-MH cells and material characterization

Commercial Co and CoO were used for all the experiments. Electrodes were made with nickel foam combined with Co or CoO mashes. The mashes were formed by mixing Co or CoO with distilled water. The electrodes were dried at 50 °C and pressed at 1 t cm^{-2}. The amount of Co in the Co-based electrode was equal to the content of Co in each positive electrode in the Co-added battery. The same conditions were used for CoO. Considering that only one-charge step was performed and that the material had to be recovered from the electrodes after charging for further analysis, no other binder (e.g., PTFE) was used. The test cells were assembled in a sandwich structure with one piece of cobalt-based electrode functioning as a positive electrode. Two commercial negative MH electrodes with a larger overcapacity than that of the cobalt-based electrode were used. The positive and negative electrodes were separated by a polypropylene separator. Similarly, a 6 M KOH solution was used as the electrolyte. Cells were then heated at 50 °C for 4 h and charged at 7 mA, the same charging current for each positive electrode of Ni/MH power batteries used in previous studies. The recorded voltages were analyzed against commercial negative MH electrodes. Every process for each of the assembled cell and all counter electrodes were identical.

After the charging, the positive electrodes were separated from the cells and immersed in distilled water for 12 h. Periodic change of the rinsing water was done to remove the remaining electrolyte in the electrodes. The cobalt materials of the positive electrodes were isolated from the nickel foam substrates with an ultrasonic oscillator, filtered, and dried.

To examine the evolution of the cobalt concentration in the electrolyte during 4 h standing in 6 M KOH solution with cobalt species, 0.13 g of CoO or 0.11 g of Co, having equal amounts of cobalt, were placed in an airtight beaker with 50 mL 6 M KOH. The beaker was heated at 50 °C for 4 h. An aliquot of 2 mL was successively taken out after 0, 1, 2, and 4 h. The aliquots were acidified and diluted with distilled water. The cobalt concentration in the ultimate solution was measured by inductively coupled plasma optical emission spectroscopy (ICP-OES, Thermo, Waltham, MA). The evolution of the cobalt concentration in the electrolyte during charging was also determined by ICP-OES. Unlike the preliminary experiments, 5% PTFE was mixed with Co or CoO to form the electrodes. It could prevent imprecise measurement of the cobalt concentration because of a loss of Co and CoO from the nickel foam. When the cell voltage reached 0.85, 0.90, 0.95, and 1.00 V during charging at 50 °C, 2 mL electrolyte was taken out at each time. This method of sampling was very convenient because only a small amount of electrolyte was needed for concentration determination every time.

The crystal structure of the cobalt materials after charging was determined by powder X-ray diffraction (XRD-6000, Shimadzu, Japan) with a Cu Kα radiation source. Electron microscopic observations were carried out using a SEM (Hitachi X-650, Japan). The nature of cobalt in the electrolyte was investigated by UV–vis absorption spectroscopy (UV-3100, Shimadzu, Tokyo, Japan).

Table 1
Practical capacities of CoO-added and Co-added batteries.

	CoO-added battery	Co-added battery
Charged capacity (Ah)	5.80	5.80
Discharged capacity (Ah)	5.52	4.90

3. Results and discussion

3.1. Electrochemical performance of CoO-added and Co-added batteries

The practical capacities of the two kinds of batteries at a 0.5 C discharging rate are listed in Table 1. The practical capacity of the CoO-added battery is significantly higher than that of the Co-added battery, indicating that the conductive network, which formed an electrical connection among the $Ni(OH)_2$ particles in the positive electrode, is better in the CoO-added battery. Thus, the CoO-added battery has a higher utilization of β-$Ni(OH)_2$ than the Co-added battery. The difference in the practical capacity of the two batteries is clarified.

In order to understand the details of the conductive network, the two kinds of batteries were discharged from a 100% state of charge at 30 C rate to a cut-off voltage of 0.7 V, followed by discharging at 0.5 C rate to a cut-off voltage of 1.0 V. The total discharge capacities (sum of the capacity of 30 C and 0.5 C rate discharges) and the voltage at the initial 0.1 s of 30 C rate discharge are shown in Table 2. The discharging performance reflects a difference in current conduction and conductive network of the batteries.

The voltage at the initial 0.1 s of 30 C rate discharge of the battery with the addition of Co is higher than that of the battery with CoO. This elucidates the better effect of the addition of Co on the electrical conduction between the $Ni(OH)_2$ particles and the nickel foam frame. This can be supported by the important influence of the ohmic internal resistance on the high rate discharge performance of the battery at the beginning of discharging.

Although the capacity of Co-added battery with a 30 C rate discharge is larger, the total discharge capacity is lower. This is consistent with the difference of practical capacity demonstrated above. From the results in Tables 1 and 2, we deduce that the addition of CoO allows for the formation of a better conductive network among the $Ni(OH)_2$ particles.

These observations show that two conductive networks can be formed in the positive electrode when Co and CoO are used as additives. One works successfully between the nickel foam frame and $Ni(OH)_2$ particles, whereas the other works well in connecting the $Ni(OH)_2$ particles themselves. As such, these two conductive networks are presumed to be constructed by different materials and to play diverse roles in improving the performance of the electrode.

3.2. Electro-oxidation process of cobalt-MH cells

In order to understand the process that the additives in the positive electrode underwent during first charging, Co-based and CoO-based electrodes were electro-oxidized with 7 mA current at 50 °C. The variations of cell voltage relative to time for each cell are presented in Fig. 1. When the starting material is CoO, oxidation occurs on a plateau at around 0.8 V vs. MH electrode. The increase of voltage after this plateau means that CoO oxidation is ending, and the oxidation of nickel foam is beginning. To avoid the interference of nickel oxidation products in the recovered sample after charging, the oxidation process was stopped at a voltage of 1.0 V.

Table 2
Performance of 30 C rate discharge of the two kinds of batteries.

	CoO-added battery	Co-added battery
Voltage at the initial 0.1 s of 30 C rate discharge	1.00 V	1.05 V
Capacity of 30 C rate discharge	0.29 Ah	2.76 Ah
Total discharged capacity	5.47 Ah	4.84 Ah

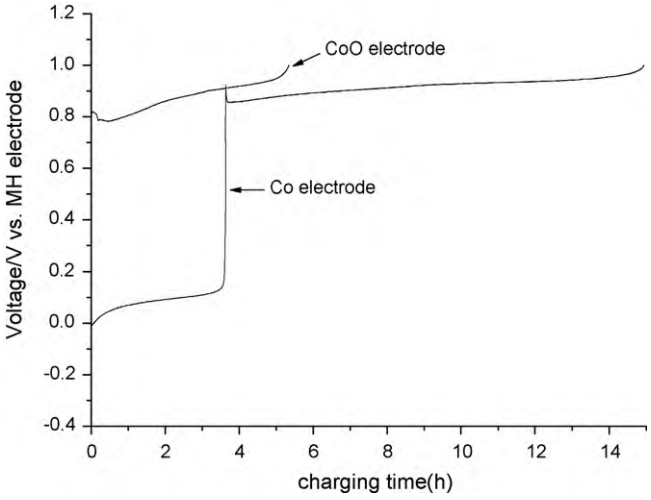

Fig. 1. Voltage evolution of Co and CoO electrodes during first charging at 50 °C in 6 M KOH solution.

The XRD patterns of the materials recovered after charging are given in Fig. 2. The curve of the material with CoO shows the formation of a pure Co_3O_4 phase, which has also been reported in an earlier report [16]. When the starting material is Co, the XRD pattern shows a mixed oxidation product comprising a CoOOH phase and a Co_3O_4 phase. The shape of the Co oxidation curve is different from that of CoO. Two oxidation plateaus can be observed at 0.1 and 0.9 V, which correspond to the oxidation of Co and subsequent oxidation of Co(II), respectively. The second oxidation plateau of Co takes place at a higher voltage than that of CoO. This is consistent with the result that the oxidation plateau of $Co(OH)_2$ is higher than the oxidation plateau of CoO [8,17].

3.3. Structural evolutions of Co and CoO during electro-oxidation

In order to study structural evolutions during the oxidation process, electrodes containing CoO were immersed in 6 M KOH

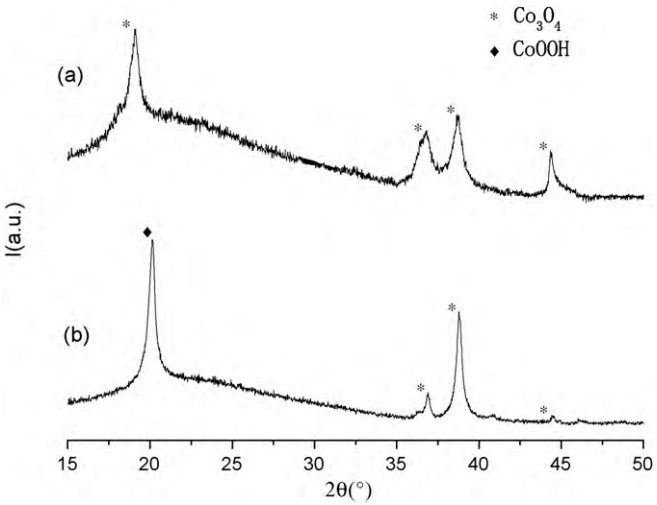

Fig. 2. XRD patterns of materials recovered after charging was stopped at 1.00 V at 50 °C: (a) from CoO and (b) from Co.

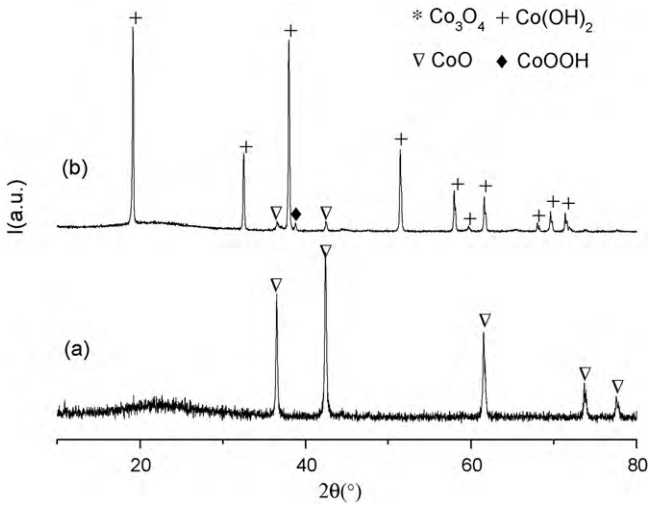

Fig. 3. (a) XRD pattern of CoO, (b) XRD pattern of the material recovered after treatment at 50 °C in 6 M KOH for 4 h from CoO.

solution at 50 °C for 4 h. Electrodes were charged in various oxidation degrees with a current of 7 mA in the same electrolyte. This was done by varying cut-off voltages during the charge process, i.e., 0.85, 0.90, 0.95, and 1.00 V. Similar electrodes containing Co were treated in the same way and charged under the same conditions. The materials were finally recovered after charging was stopped.

With CoO as the starting material, XRD patterns of the recovered materials before and after standing in 6 M KOH for 4 h at 50 °C are displayed in Fig. 3. After 4 h of treatment, some CoO transforms to $Co(OH)_2$, whereas some CoO remains unchanged. Small quantities of CoOOH and Co_3O_4 have been formed through this process. These two materials probably result from the oxidation of CoO by the oxygen molecules dissolved in the electrolyte.

When the starting material is CoO, the XRD patterns of the recovered materials with different oxidation degrees are shown in Fig. 4. The cut-off voltage during the oxidation process was raised, and the amount of $Co(OH)_2$ was gradually reduced. An increase in the quantity of Co_3O_4 is observed. In the end, no CoOOH material remains.

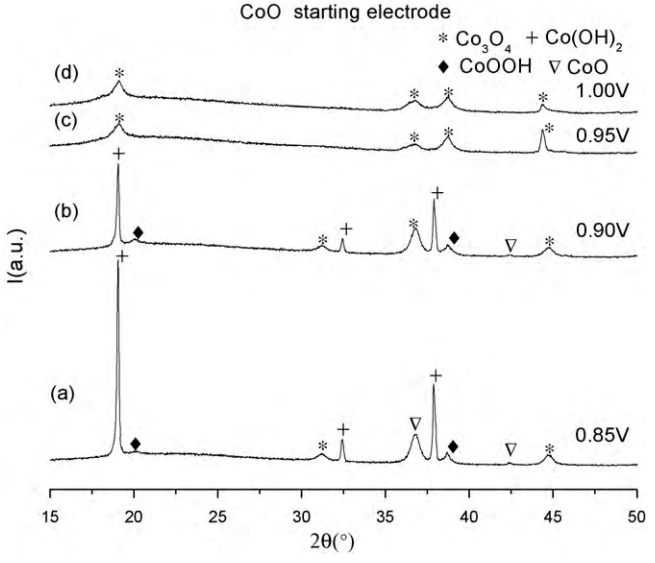

Fig. 4. XRD patterns of the CoO-based materials recovered after charging was stopped at: (a) 0.85 V, (b) 0.90 V, (c) 0.95 V, and (d) 1.00 V.

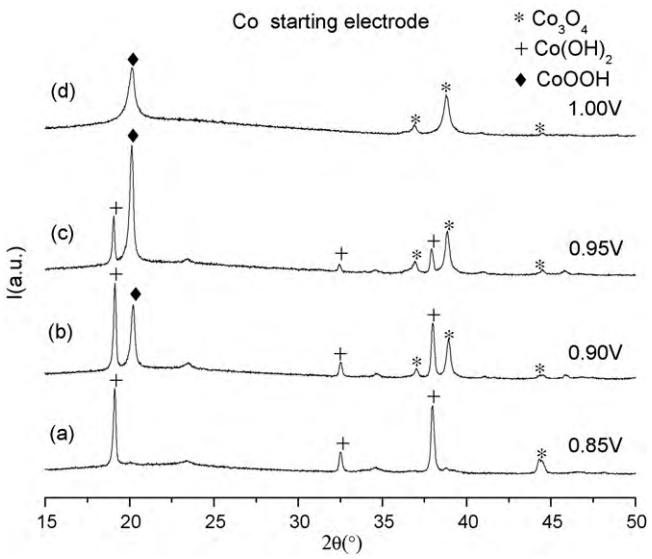

Fig. 5. XRD patterns of the Co-based materials recovered after charging was stopped at: (a) 0.85 V, (b) 0.90 V, (c) 0.95 V, and (d) 1.00 V.

Moreover, $Co(OH)_2$ is completely oxidized to Co_3O_4 before the cell voltage reached 0.95 V (Fig. 4c). In Fig. 4 c and d, the crystallinity of Co_3O_4, formed by electro-oxidation, is poor. However, based on the capacitive performance of the Ni/MH power battery, utilization of β-$Ni(OH)_2$ is high. This indicates the excellent conductivity of this type of Co_3O_4.

Most of the starting Co does not change during 4 h in 6 M KOH at 50 °C. Only a small amount of $Co(OH)_2$ appears (result not presented here). The XRD patterns of the recovered materials with different oxidation degrees are shown in Fig. 5. When the cut-off voltage is set at 0.85 V, no Co material remains. Co is completely oxidized to $Co(OH)_2$ before the cell voltage reaches 0.85 V. The amounts of CoOOH and Co_3O_4 gradually increase during the whole charging process, whereas the amount of $Co(OH)_2$ is gradually reduced. Both the CoOOH and Co_3O_4 phases are present in the final material when the cut-off voltage is set at 1.00 V. An interesting observation is the remaining amount of $Co(OH)_2$ when the cut-off voltage is set at 0.95 V during charging because this means that the oxidation of $Co(OH)_2$ still proceeds at 0.95 V. This is not the case for CoO. This is consistent with the result where the second oxidation plateau of Co is higher than the oxidation plateau of CoO (Fig. 1). This implies that the oxidation polarization of $Co(OH)_2$ formed by the oxidation of Co is greater than the oxidation polarization of $Co(OH)_2$ formed by the hydrolysis of CoO. This is consistent with an earlier work, which has shown that the oxidation polarization of $Co(OH)_2$ is greater than the oxidation polarization of $Co(OH)_2$ formed by the hydrolysis of CoO [17].

These behaviors raise questions with regard to the reasons for the differences in the oxidation products as well as the role of CoOOH in the oxidation process. CoOOH is present in the sample at the end of charging when the starting material is Co but does not exist when the starting material is CoO. This can possibly be explained by the oxidation mechanism. In addition, some observations on the electrolyte could be employed to clarify the oxidation mechanism.

3.4. Cobalt complex in the electrolyte

In order to clarify the form of the cobalt complex that exists in the electrolyte and whether it takes part in cobalt oxidation, the cobalt species dissolved in the electrolyte were investigated. The

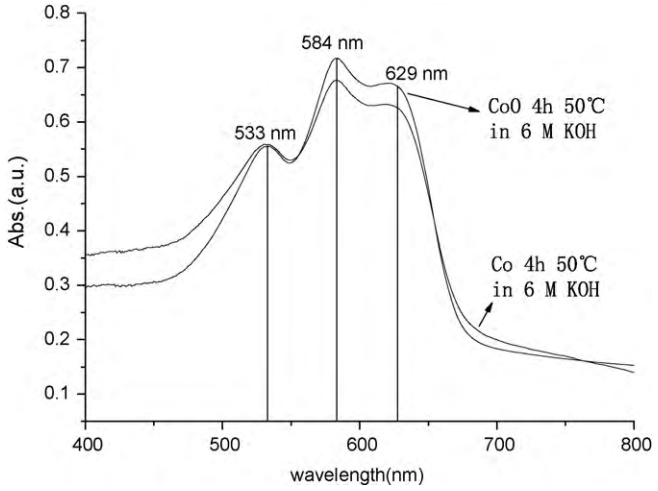

Fig. 6. UV–vis spectra of solutions sampled after Co and CoO were immersed in 6 M KOH solution at 50 °C for 4 h.

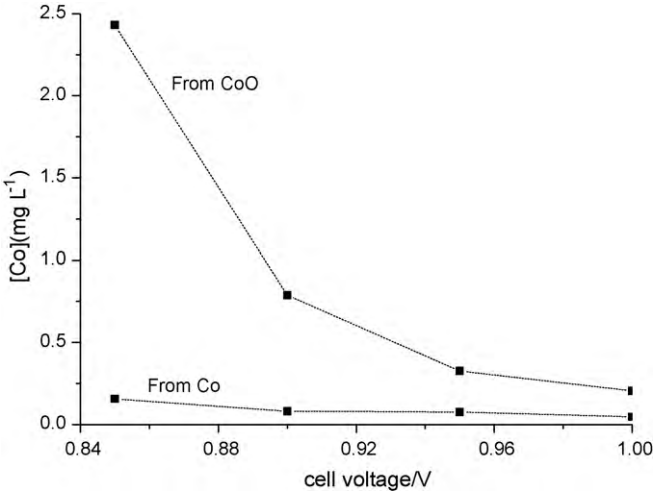

Fig. 8. Evolution of the concentration of cobalt in the electrolyte vs. cell voltage during charging of Co-based electrode and of CoO-based electrode.

change in the color of the solution during charging as well as with the structural evolutions merited more investigation.

Before charging, the electrolyte has a weak blue color, consistent with the color of a cobalt complex in alkaline solution [11]. When the charging time increased, the electrolyte solution gradually became colorless. UV–vis spectroscopy experiments were performed on the electrolyte solutions. The spectra obtained after Co and CoO were immersed in 6 M KOH solution at 50 °C for 4 h are presented in Fig. 6. The two curves show almost the same trend for the three absorption peaks at 533, 584, and 629 nm, which affirm that the blue cobalt complex involved is cobalt tetrahydroxide $[Co(OH)_4]^{2-}$ [11,17].

Since $Co(OH)_4^{2-}$ is possibly related to the cobalt oxidation mechanism, it is important to examine the evolution of the cobalt concentration in the electrolyte during the whole process. The evolution of the cobalt concentration as a function of standing time is presented in Fig. 7. Cobalt concentration increases regularly with standing time, and the amount of cobalt in the solution is higher when the material is CoO rather than Co. The hydrolysis of CoO followed by the dissolution of $Co(OH)_2$ at 50 °C may be the possible reason behind this observation. However, a small part of the starting Co can be oxidized to $Co(OH)_2$ by the oxygen molecules dissolved in the alkaline solution. This is also followed by the dissolution of $Co(OH)_2$ at 50 °C.

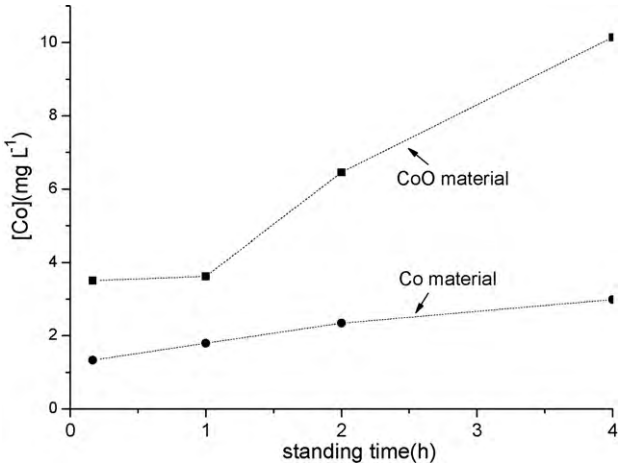

Fig. 7. Evolution of the cobalt concentration in the electrolyte vs. standing time in 6 M KOH at 50 °C with CoO and Co as starting materials.

The evolution of the cobalt concentration in the electrolyte during charging was further determined. The results of the evolution of cobalt concentration in the electrolyte vs. the cell voltage are shown in Fig. 8. Cobalt concentration in the electrolyte decreases during the whole charging process whether the starting material is Co or CoO. The cobalt concentration drops from 2.43 to 0.20 mg L^{-1} when the starting material is CoO, whereas it drops from 0.15 to 0.05 mg L^{-1} when the starting material is Co. This indicates that the cobalt complex is consumed during charging; that is, $Co(OH)_4^{2-}$ species is consumed during the oxidation. This probably corresponds to the reaction between CoOOH and $Co(OH)_4^{2-}$ [17]. Furthermore, this reaction explains exactly why the CoOOH phase disappears during charging when the starting material is CoO (Fig. 4).

3.5. Texture of the cobalt materials

SEM images of Co and CoO before and after charging are illustrated in Fig. 9. A substantial change in the materials during the oxidation process of both Co and CoO is observed. When the starting material is CoO, $Co(OH)_2$ forms cube-like particles (Fig. 9a-1), which are made up of stacks of nano-particles (Fig. 9a-2), after 4 h standing in 6 M KOH at 50 °C (Fig. 3b). This suggests that the hydrolysis step occurs through a dissolution-reprecipitation process in the electrolyte. After charging was stopped at 1.00 V, the material still exhibits the morphology of tiny particles. The XRD pattern of the corresponding material presented in Fig. 4d shows that the material obtained from CoO consists of Co_3O_4. Thus, crystals comprised of tiny particles are Co_3O_4.

When the starting material is Co, standing for 4 h in 6 M KOH at 50 °C does not significantly change the texture of Co. A hexagonal plate-like morphology is still observed. This is consistent with the XRD result described in the previous section. It is noteworthy that the particle size of Co is much bigger than the particle size of $Co(OH)_2$ formed by the hydrolysis of CoO (Fig. 9a-2 and c-2). After charging was stopped at 1.00 V, the material maintains a plate-like morphology. This is different from the image of the oxidized product of CoO.

The cross-sections of the electrodes surrounding the nickel foam frame, with Co and CoO as the starting materials, at the point where the charging was stopped at 1.00 V are illustrated in Fig. 10.

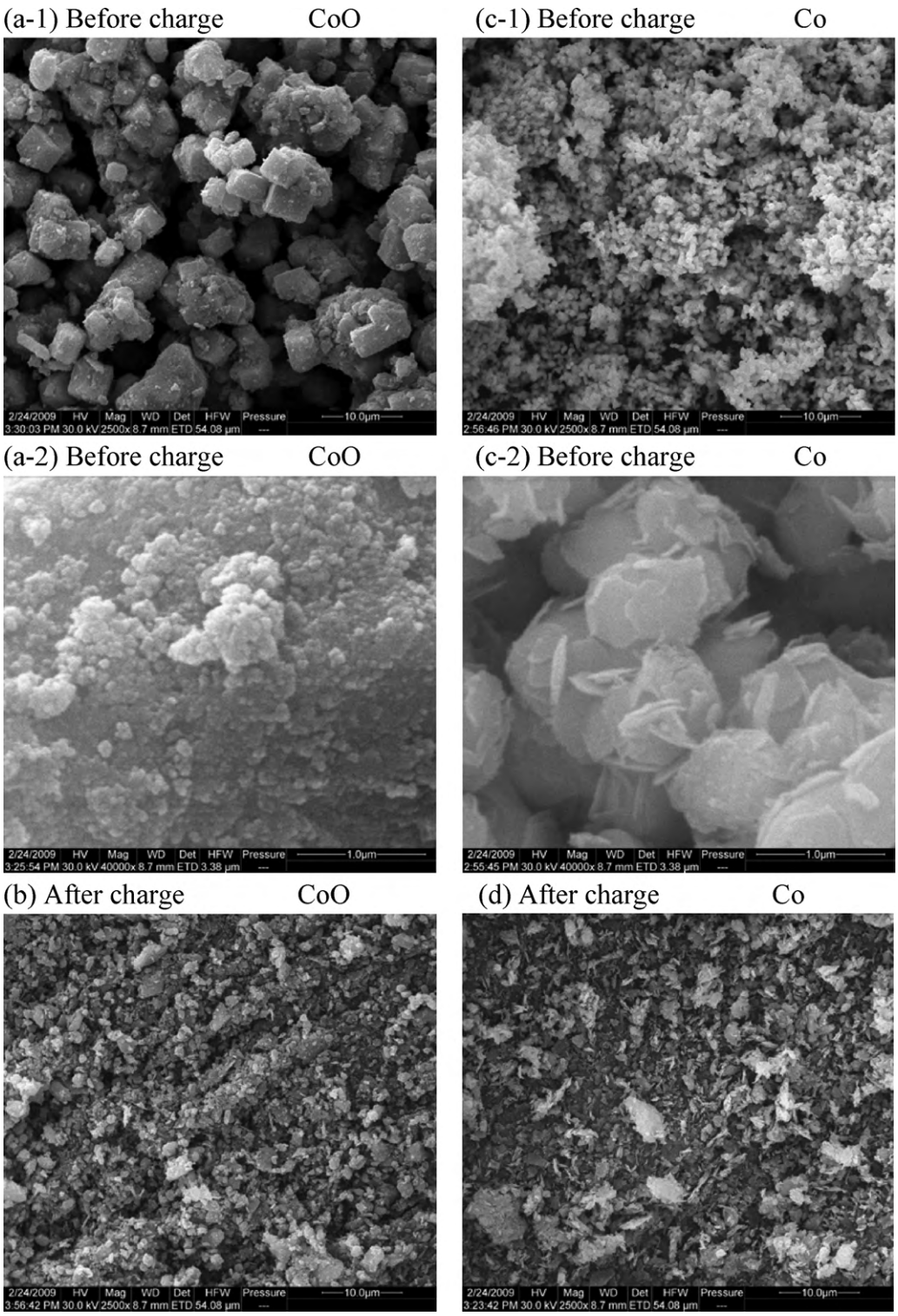

Fig. 9. SEM images: (a-1) CoO after 4 h standing in 6 M KOH at 50 °C (2500×), (a-2) CoO after 4 h standing in 6 M KOH at 50 °C (40000×), (b) CoO after charging was stopped at 1.00 V (2500×), (c-1) Co after 4 h standing in 6 M KOH at 50 °C (2500×), (c-2) Co after 4 h standing in 6 M KOH at 50 °C (40,000×), (d) Co after charging was stopped at 1.00 V (2500×).

The phase attached to the nickel foam is comprised one layer when the starting material is CoO and two layers when the starting material is Co. The texture of the single layer observed from CoO is similar to the external layer observed from Co. The XRD pattern of the corresponding material (Fig. 4d) shows that only one phase is made of Co_3O_4. Therefore, considering the result shown in Fig. 4d, the layer observed from CoO (Fig. 10a) should be Co_3O_4.

When the starting material is Co, two layers are observed in the cross-section of the electrode (Fig. 10b). The external layer, similar to the layer observed in the CoO electrode, is determined as Co_3O_4. The layer closer to the nickel foam frame is composed of a plate-like phase, where the particles are gathered in a highly compact manner. Considering the XRD result (Fig. 5d), this phase can be designated as CoOOH. Observations on the SEM images agree with the XRD results well.

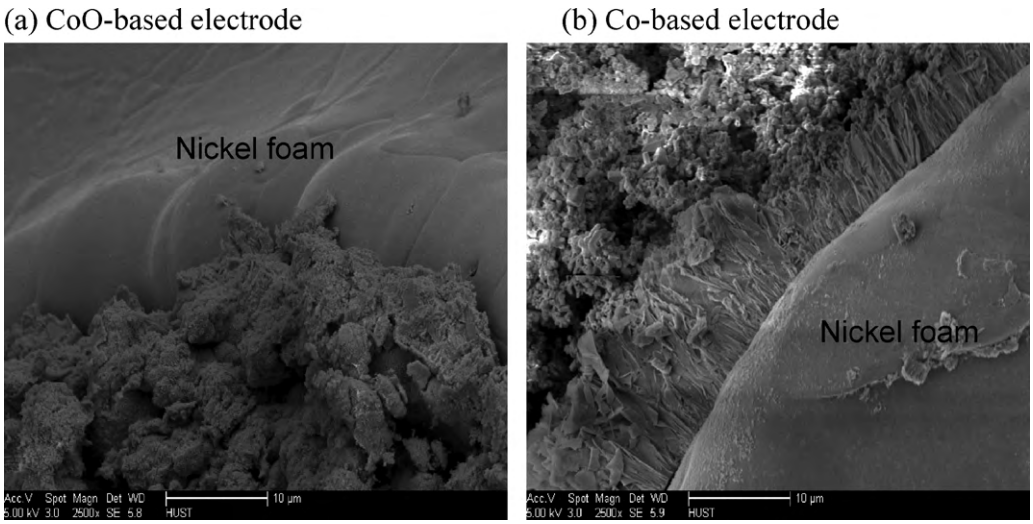

Fig. 10. SEM images of the cross-sections of the electrodes; area is close to the nickel foam captured after charging was stopped at 1.00 V: (a) CoO-based electrode and (b) Co-based electrode.

3.6. Cobalt oxidation mechanism

To explain the effects of the two cobalt additives on the Ni/MH power battery and their structural and textural evolutions during first charging, the electro-oxidation mechanism of Co and CoO is proposed according to the previous results. When the starting material is Co, it is initially electro-oxidized to $Co(OH)_2$, which corresponds to the first plateau of Co oxidation in Fig. 1. The reaction can be written as [19]:

$$Co + 2OH^- \rightarrow Co(OH)_2 + 2e^-. \quad (1)$$

The cobalt complex dissolved in the electrolyte is confirmed in this study. Thus, the dissolution of $Co(OH)_2$ in concentrated KOH solution should correspond to the reaction:

$$Co(OH)_2 + 2OH^- \rightarrow Co(OH)_4^{2-}. \quad (2)$$

At the same time, the cobalt material, $Co(OH)_2$, can proceed through a classical electrochemical oxidation, from $Co(OH)_2$ to CoOOH [3,6]. The resulting CoOOH can further react with the cobalt complex in the electrolyte [17]. These two reactions can be expressed by the following equations:

$$Co(OH)_2 + OH^- \rightarrow CoOOH + H_2O + e^-. \quad (3)$$

$$Co(OH)_4^{2-} + 2CoOOH \rightarrow Co_3O_4 + 2H_2O + 2OH^-. \quad (4)$$

When the starting material is CoO, it is initially hydrolyzed into $Co(OH)_2$ according to the following equation:

$$CoO + H_2O \rightarrow Co(OH)_2. \quad (5)$$

Then, it proceeds to reactions (2), (3) and (4).

Although the reaction processes are almost the same when Co or CoO is used as the starting material, the oxidation products are different. The amounts of Co_3O_4 and CoOOH are significantly influenced by the solubility of cobalt and the kinetics of reactions (3) and (4). A higher solubility of cobalt leads to a bigger amount of Co_3O_4 produced. The concentration of $Co(OH)_4^{2-}$ is higher when CoO is used as a starting material (Figs. 7 and 8). This leads to a higher amount of Co_3O_4, according to the cobalt oxidation mechanism. This deduction is consistent with the XRD patterns shown in Figs. 4d and 5d. In addition, the hydrolysis of CoO shown in Eq. (5) is more likely to form much smaller particles of $Co(OH)_2$ rather than Co (Fig. 9a-2 and c-2). Smaller $Co(OH)_2$ particles lead to smaller CoOOH particles. Since the smaller particles have larger specific surface areas, their electrochemical polarization is lower than the electrochemical polarization of bigger particles in the reaction. This reason explains why the oxidation plateau of smaller particles is lower than the oxidation plateau of bigger particles in the oxidation reaction. This is the reason why the oxidation plateau voltage for the CoO electrode is lower than the second oxidation plateau voltage for the Co electrode in Fig. 1.

A schematic illustration of the charge processes of electrodes with Co or CoO as the starting materials at 50 °C are shown in Fig. 11. This can be used to explain the change in the material compositions and the morphologies of the electrodes. When the starting material is CoO, the formation of CoOOH first appears near the nickel foam. The formed CoOOH is then transformed into Co_3O_4, and the successive CoOOH is formed further away from the nickel foam until the $Co(OH)_2$ is fully used up. Finally, all the earlier formed CoOOH is transformed into Co_3O_4. However, a different process is observed when Co is the starting material. Earlier formed CoOOH is close to the nickel foam. It cannot be transformed into Co_3O_4 because $Co(OH)_4^{2-}$ cannot penetrate the highly compact phase (Fig. 10b). Only CoOOH forms at a latter stage at a distance from the nickel foam, and the not highly compact phase can be transformed into Co_3O_4. Moreover, the lower concentration of $Co(OH)_4^{2-}$ and the bigger particle size of CoOOH are possible reasons for this result.

This mechanism can also explain the decrease of $Co(OH)_4^{2-}$ concentration in the electrolyte as a result of its consumption in Eq. (4). This mechanism can be used to account for the materials needed to construct the two conductive networks in the positive electrode of Ni/MH power battery.

3.7. Two conductive networks in $Ni(OH)_2$ electrode

The positive electrodes from the two kinds of Ni/MH power batteries were analyzed by SEM after testing. The cross-sections of the positive electrodes close to the nickel foam recovered from the Co-added and CoO-added cells are presented in Fig. 12. When the additive is Co, the layer close to the nickel foam has a highly compact form composed of platelet-type particles. This is very similar to the layer close to the nickel foam shown in Fig. 10b. We deduce that the highly compact phase should be an effective conductive network for the nickel foam and $Ni(OH)_2$ particles, especially at high charge and discharge rates.

XRD and SEM show that the layer that formed close to the nickel foam is Co_3O_4 when the additive is CoO. In Fig. 12b, however, the surface layer has been changed to a flimsy layer, which consists

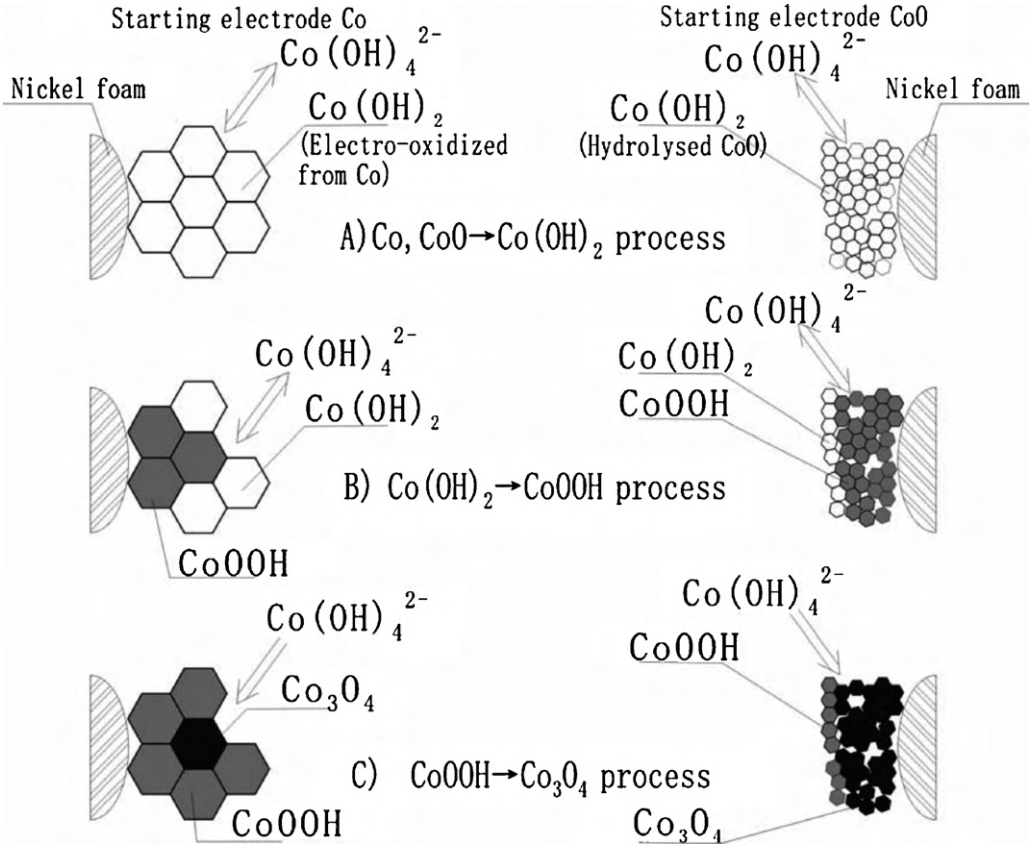

Fig. 11. Schematic illustration of the processes involved during charging at 50 °C of the electrode containing Co or CoO: (a) textural differences between $Co(OH)_2$ electro-oxidized from Co and $Co(OH)_2$ hydrolyzed from CoO, (b) electro-oxidation process of $Co(OH)_2$ transformation into CoOOH, (c) reaction process of CoOOH transformation into Co_3O_4.

of thin foils, after the cycling test of the positive electrode. This is probably caused by the oxygen-evolution reaction, which happens at the end of electrode charging [17]. This phase is believed to have a worse effect on the connection between the nickel foam and $Ni(OH)_2$ particles than the highly compact phase (Fig. 12a).

On the basis of these observations, it can be concluded that the conductive network, which works successfully in connecting the nickel foam and $Ni(OH)_2$ particles in the Co-added battery, must be the CoOOH phase. The conductive network, which works well in connecting the $Ni(OH)_2$ particles among themselves in the CoO-added battery, must be the Co_3O_4 phase. If only Co is used as an additive, the oxidation process has a weak dissolution-reprecipitation reaction via the electrolyte. Consequently, it has a worse distribution of cobalt within the electrode than the battery with CoO additive. This leads to the lower utilization of β-$Ni(OH)_2$ in the Co-added battery. When only CoO is used as additive, the highly compact CoOOH phase, which has a better effect than the Co_3O_4 phase in connecting the nickel foam and $Ni(OH)_2$ particles, cannot be obtained during first charging. The CoO-added battery is not qualified as a power battery on account of its poor capabil-

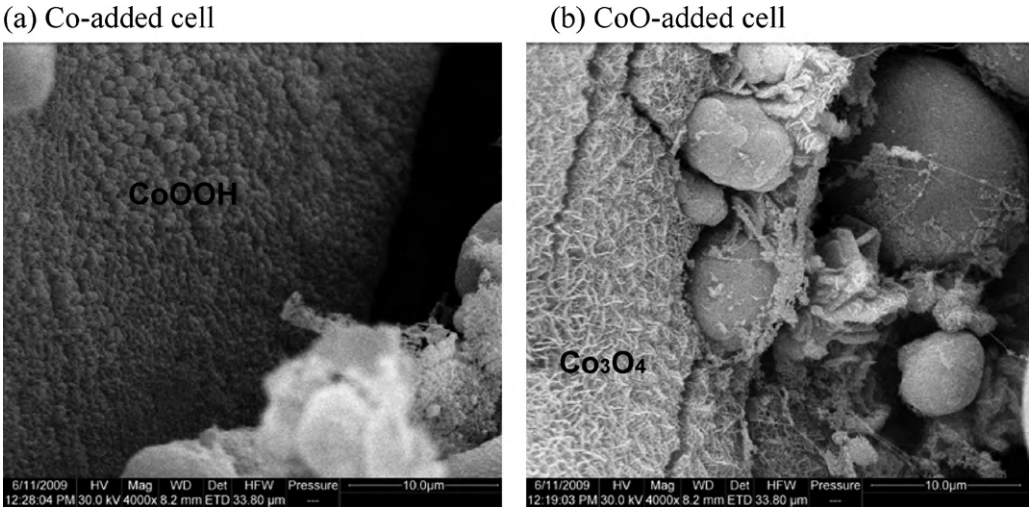

Fig. 12. SEM images of the cross-sections of the positive electrodes; area is close to the nickel foam and taken after testing: (a) Co-added cell, (b) CoO-added cell.

ity for high rate charge and discharge. Fortunately, the CoO-added battery and Co-added battery have reciprocal characteristics. Thus, both CoO and Co are necessary additives to the positive electrode to create the Ni/MH power battery.

4. Conclusions

We have reported the electrochemical behavior of Co and CoO as additives in the positive electrode of Ni/MH power batteries in an alkaline medium during first charging at 50 °C. The structural and textural evolutions of Co and CoO during charging were studied, and an oxidation mechanism was proposed. Moreover, the effects of the two additives in the positive electrode on the performance of Ni/MH power batteries were investigated. The following conclusions were reached:

1. Different oxidation products could be obtained according to the kind of starting material. When the starting material was CoO, only Co_3O_4 was formed. A CoOOH phase was present together with a Co_3O_4 phase when Co was used as a starting material.
2. The oxidation mechanism of Co and CoO revealed that two factors, the solubility of cobalt and kinetics of the reaction that consumes CoOOH, could significantly influence the amounts of Co_3O_4 and the remaining CoOOH. The $Co(OH)_4^{2-}$ concentration decreased simultaneously during charging for both Co and CoO.
3. According to the electrochemical performance of the CoO-added and Co-added batteries and the cobalt oxidation behavior, the highly compact CoOOH phase, which worked well in connecting the nickel foam and $Ni(OH)_2$ particles, enhanced the high rate charge and discharge performance of the Ni/MH power battery. The Co_3O_4 phase, which worked well in connecting $Ni(OH)_2$ particles with each other, increased the utilization of β-$Ni(OH)_2$, consequently improving the capacitive performance of the Ni/MH power battery. Therefore, both additives are necessary to create a power battery.

Acknowledgement

The financial support by the 863 National Research and Development Project Foundation of China (Grant No. 2006AA11A152) is gratefully acknowledged.

References

[1] D. Ohms, M. Kohlhase, G. Benczúr-Ürmössy, G. Schädlich, J. Power Sources 105 (2002) 127.
[2] J. Chen, D.H. Bradhurst, S.X. Dou, H.K. Liu, J. Electrochem. Soc. 146 (1999) 3606.
[3] V. Pralong, A. Delahaye-Vidal, B. Beaudoin, B. Gérand, J.M. Tarascon, J. Mater. Chem. 9 (1999) 955.
[4] A. Audemer, A. Delahaye, R. Farhi, N. Sac-Epée, J.-M. Tarascon, J. Electrochem. Soc. 144 (1997) 2614.
[5] M. Oshitani, H. Yufu, K. Takashima, S. Tsuji, Y. Matsumaru, J. Electrochem. Soc. 136 (6) (1989) 1590.
[6] P. Benson, G.W.D. Briggs, W.F.K. Wynne-Jones, Electrochim. Acta 9 (1964) 275.
[7] M. Butel, L. Gautier, C. Delmas, Solid State Ionics 122 (1999) 271.
[8] V. Pralong, A. Delahaye-Vidal, B. Beaudoin, J.B. Leriche, J.M. Tarascon, J. Electrochem. Soc. 147 (4) (2000) 1306.
[9] L. Gautier, Ph.D. Thesis, Bordeaux I, France (1995).
[10] M. Butel, Ph.D. Thesis, Bordeaux I, France (1998).
[11] V. Pralong, A. Delahaye Vidal, B. Beaudoin, J.B. Leriche, J. Scoyer, J.M. Tarascon, J. Electrochem. Soc. 147 (6) (2000) 2096.
[12] A.H. Zimmerman, R. Seaver, J. Electrochem. Soc. 137 (9) (1990) 2662.
[13] S. Aravamuthen, C.V. Annamma, N.R. Pillai, M.J. Nair, J. Power Sources 50 (1994) 81.
[14] K. Yuasa, Japanese Patent, JP 2003-031216 (2003).
[15] D. Furukawa, Japanese Patent, JP 330858/95 (1995).
[16] F. Tronel, L. Guerlou-Demourgues, M. Ménétrier, L. Croguennec, L. Goubault, P. Bernard, C. Delmas, Chem. Mater. 18 (25) (2006) 5840.
[17] F. Tronel, L. Guerlou-Demourgues, L. Goubault, P. Bernard, C. Delmas, J. Power Sources 179 (2008) 837.
[18] M. Douin, L. Guerlou-Demourgues, M. Ménétrier, E. Bekaert, L. Goubault, P. Bernard, C. Delmas, Chem. Mater. 20 (2008) 6880.
[19] A. Yuan, S. Cheng, J. Zhang, C. Cao, J. Power Sources 77 (1999) 178.